

Localization of Epidermal Growth Factor (EGF) Binding Sites on Antiluminal Plasma Membrane of Rat Kidney: Autoradiographic Study Using Nonfiltering Perfused Rat Kidney

Dong Chool Kim,¹ Yuichi Sugiyama,^{1,3}
Yasushi Kanai,² Norio Ohnuma,² and
Manabu Hanano¹

Received April 23, 1991; accepted July 10, 1991

We previously demonstrated that the specific binding of EGF to the antiluminal plasma membrane was a prerequisite step for the renal uptake of EGF. In the present study, the localization of ¹²⁵I-EGF binding sites on the antiluminal plasma membrane was investigated by tissue sampling and X-ray autoradiography in the nonfiltering kidney. The binding of ¹²⁵I-EGF was recognized over the whole kidney and was highest in the inner medulla followed by the cortex and outer medulla. The binding of ¹²⁵I-EGF in the nonfiltering kidney was completely inhibited in the presence of 20 nM unlabeled EGF, suggesting specific binding of ¹²⁵I-EGF to its receptor. Further, we used a histologic tissue staining method to confirm the location of the ¹²⁵I-EGF binding sites. Binding of ¹²⁵I-EGF was demonstrated on the proximal straight tubules (PST), cortical collecting ducts (CCD), inner medullary collecting ducts (IMCD), and thin limb of Henle in the inner medulla (IMTLH). We found that the binding of ¹²⁵I-EGF was high in the IMTLH. In addition, we determined the grain density both on the cell surface membrane and in the intracellular space of the proximal straight tubules, where the grain density on the antiluminal plasma membrane was approximately 50% that in the intracellular space at 20 min after the start of ¹²⁵I-EGF perfusion, suggesting the internalization of ¹²⁵I-EGF from the antiluminal plasma membrane to the intracellular compartment. In conclusion, the binding sites of ¹²⁵I-EGF, which were accessible from the antiluminal side, were broadly distributed over the whole kidney and were most dense around the IMTLH.

KEY WORDS: epidermal growth factor (EGF); kidney perfusion; autoradiography; binding; antiluminal membrane.

INTRODUCTION

We previously demonstrated that kidney as well as liver plays an important role in the elimination of EGF from the circulating plasma after its iv administration (1–4). Subsequently, the specific binding of EGF to the antiluminal plasma membrane was suggested to be a prerequisite step for the renal uptake of EGF (5). The kidney has been shown as a major site of synthesis of the EGF precursor, prepro-EGF (6), and a considerable amount of EGF has been found in

human urine (7). The cortical thick ascending limb and distal convoluted tubule were shown to be rich in mRNA for prepro-EGF (8,9), and EGF peptides from the above tubules are thought to be excreted into the urine (10). Various nephron segments are reported as the target tissues for EGF (11). Sack and Talor (12) demonstrated specific binding of EGF to antiluminal membrane vesicles isolated from the cortex of rabbit kidney but not to luminal membrane vesicles.

Using isolated perfused rat kidney (filtering and nonfiltering), we previously estimated the relative contribution of two uptake routes to the total renal uptake of EGF, one being the luminal uptake (reabsorption) of EGF after glomerular filtration and the other the receptor-mediated endocytosis (RME) of EGF through the antiluminal plasma membrane. The contribution of RME through the antiluminal plasma membrane was shown to be more important (5,13). Based on Scatchard analysis of cell surface bound EGF obtained at various concentrations of EGF in the nonfiltering kidney, two binding sites with differing affinities ($K_{d1} = 0.1$ nM, $K_{d2} = 25$ nM) were identified on the kidney antiluminal plasma membrane (13). No information on the intrarenal distribution of EGF binding sites on the antiluminal plasma membrane of the kidney is available so far. EGF binding sites were found on rat proximal tubule (14), mesangial cells (15), and cortical collecting ducts (16). But in these studies, EGF receptors were identified using binding assays or by the observation of biological effects of EGF on those isolated nephron segments. There are few studies investigating the relative density of EGF binding sites along the nephron. In the present study, we therefore tried to investigate the localization and relative density of EGF binding sites on the antiluminal plasma membrane of the nonfiltering kidney employing autoradiography.

MATERIALS AND METHODS

Materials

Biosynthetic human epidermal growth factor (EGF), obtained from *Escherichia coli* via a previously described synthesized coding sequence (17), was used in all experiments. Sodium iodide-125 (100 mCi/ml) was purchased from the Radiochemical Center (Amersham Corp., Arlington Heights, IL). The EGF was radiolabeled with ¹²⁵I-Na by the chloramine-T method (18). Unreacted ¹²⁵I-Na was removed with a Sephadex G-25 column, and the ¹²⁵I-EGF was eluted in the void volume. The ¹²⁵I-EGF had a specific activity of 0.5 to 1.0 mCi/mol. Bovine serum albumin (fraction V) was purchased from Sigma, and all other chemicals were obtained from commercial sources and were of analytical grade.

Nonfiltering Isolated Perfused Rat Kidney

The isolated perfused rat kidney technique previously described by our laboratory (19) has been slightly modified. After male Wistar rats weighing 300–380 g were anesthetized with ether, the renal artery was cannulated via the mesentric artery without interruption of blood flow. The renal vein was also cannulated. An 18-gauge needle connected to silicon tubing (ID, 3 mm; OD, 5 mm) was used for the renal arterial

¹ Faculty of Pharmaceutical Sciences, University of Tokyo, Hongo, Bunkyo-ku, Tokyo 113; Japan.

² Clinical Pharmacology and Biochemistry Laboratory, Suntory Bio-Pharma Tech Center, 2716-1 Chiyoda-machi, Ohra-gun, Gunma 370-5, Japan.

³ To whom correspondence should be addressed.

,cannula, polyethylene tubing (ID, 2 mm; OD, 3 mm) for the renal vein cannula. The perfusate composition is as follows: Krebs–Henseleit buffer (NaCl, 116 mM; KCl, 4 mM; CaCl₂, 2 mM; KH₂PO₄, 1.5 mM; MgSO₄, 2.4 mM; NaHCO₃, 25 mM) containing fraction V bovine serum albumin (10 g/dl), glucose (1 mg/ml), and a mixture of amino acids (*l*-methionine, 0.5 mM; *l*-alanine, 2 mM; glycine, 2 mM; *l*-serine, 2 mM; *l*-proline, 2 mM; *l*-isoleucine, 1 mM; *l*-aspartic acid, 3 mM; *l*-arginine, 1 mM; *l*-cysteine, 0.5 mM; *l*-glutamate, 0.5 mM) (20,21). Monoiodotyrosine (1 mM) was included in perfusions containing ¹²⁵I-EGF to inhibit deiodination of degradation products (22). Immediately after the operation on the right kidney, it was excised and perfused in a closed-circuit system. Unless otherwise noted, kidneys were perfused at 37°C with 100 ml of perfusate. The perfusate was continuously gassed with a mixture of 95% O₂–5% CO₂, and its pH adjusted to 7.4. The effective perfusion pressure was approximately 85 mm Hg, with a perfusate flow rate of 17–21 ml/min/kidney.

Intrarenal Distribution of EGF Binding Sites in the Nonfiltering Kidney

Tissue Sampling Method. After a 20-min recirculatory perfusion of various concentrations of EGF (tracer ¹²⁵I-EGF only or tracer ¹²⁵I-EGF plus 0.5 nM or 20 nM unlabeled EGF) in the nonfiltering kidney, the perfusion medium was switched to buffer (pH 7.4) free of EGF and perfused for an additional 5 min to wash out the ¹²⁵I-EGF remaining in the extracellular space. During the recirculatory perfusion of EGF, the perfusion medium was sampled from the reservoir at designated times (0, 5, 10, 15, 20 min), and its TCA-precipitable ¹²⁵I-radioactivity was ascertained in a gamma counter. After the buffer washing procedure, the perfused kidney was dissected into cortex, outer medulla, and inner medulla and the wet weight of each section was measured. Dissection was performed on an ice-cooled petri dish. The sections were assayed for ¹²⁵I-radioactivity in a gamma counter (Model ARC-300, Aloka Co., Ltd., Tokyo).

Autoradiographic Studies. After a 20-min recirculatory perfusion of tracer ¹²⁵I-EGF, the perfusion medium was switched to buffer (pH 7.4) free of EGF and perfused for an additional 5 min to wash out the ¹²⁵I-EGF remaining in the extracellular space, and then the perfusion medium was again changed to 2% glutaraldehyde saline solution and perfused for 5 min with the perfusate flow rate of 5 ml/min/kidney. The perfused kidney was preserved overnight in 2% glutaraldehyde saline solution and then dehydrated by means of a serial treatment of ethanol solutions from 50 to 100% and, finally, preserved in 100% xylene until dissection. The paraffin sections (20 μm thick) prepared from the dehydrated nonfiltering kidney were mounted on glass slides and dried. The X-ray films (IX-150, Fuji Film, Tokyo) were tightly apposed to the sections, exposed for 60 days at 4°C, and developed to allow for the quantitative measurement of density (23). The densities of enlarged autoradiographic images were measured with a image analyzer (IBAS, Carl Zeiss, Germany) that converts the amount of light into gray values. The tissue radioactivity was estimated by means of standards for autoradiography.

To observe the binding sites of ¹²⁵I-EGF histologically

at the microscopic level, some paraffin sections (4 μm in thickness) were mounted on glass slides and dipped into nuclear track emulsion (NTB-2, Eastman Kodak) and exposed for 60 days. After preparations were developed and fixed, they were stained with hematoxylin–eosin and the silver grains were counted with the use of the image analyzer.

RESULTS

During the 20-min recirculatory perfusion of a tracer amount of ¹²⁵I-EGF in the nonfiltering kidney (100 ml of perfusate), the TCA-precipitable radioactivities per milliliter of the perfusate decreased by less than 3% of the initial value, representing a minimal clearance of ¹²⁵I-EGF. In parallel, the fraction of TCA-soluble radioactivity increased only by 2.3% during the perfusion, indicating minimal degradation of ¹²⁵I-EGF to small fragments. After ¹²⁵I-EGF tracer perfusion for 20 min, the level of ¹²⁵I-radioactivity determined by the tissue sampling method was highest in the inner medulla. The ¹²⁵I-EGF distribution was similar between the cortex and the outer medulla (Fig. 1). The binding of ¹²⁵I-radioactivity to those sites was almost completely inhibited by the addition of excess unlabeled EGF (20 nM) in the perfusate (Fig. 1). When the perfusate concentration of EGF was 0.5 nM, the binding of ¹²⁵I-EGF was inhibited by 45–55%, as compared to the tracer ¹²⁵I-EGF experiment in the cortex and outer medulla. On the other hand, the presence of 0.5 nM unlabeled EGF only slightly inhibited the binding of ¹²⁵I-EGF in the inner medulla, which was approximately 75% of that in the tracer ¹²⁵I-EGF experiment.

Figure 2 shows the distribution of ¹²⁵I-EGF binding sites, as determined by autoradiography 20 min after the recirculatory perfusion of tracer ¹²⁵I-EGF in the nonfiltering kidney, and the results of quantitative analysis of the autoradiographs are summarized in Table I. Sites with high and low optical densities were observed within the cortex (Fig. 2). The gradient of optical density representing the distribution of ¹²⁵I-EGF binding was inner medulla > cortex ~ outer

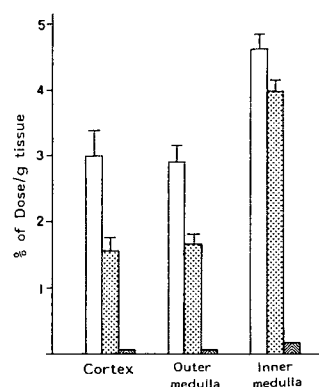


Fig. 1. Intrarenal distribution of ¹²⁵I-radioactivity in the nonfiltering kidney. The nonfiltering kidneys were perfused with a tracer amount of ¹²⁵I-EGF or together with unlabeled EGF (0.5 or 20 nM) during a 20-min period. After the recirculatory perfusion, the kidneys were dissected into cortex, outer medulla, and inner medulla and the ¹²⁵I-radioactivity in each fraction was determined. The perfusate concentrations of EGF are as follows: open bar, tracer ¹²⁵I-EGF; dotted bar, ¹²⁵I-EGF plus 0.5 nM unlabeled EGF; hatched bar, ¹²⁵I-EGF plus 20 nM unlabeled EGF.

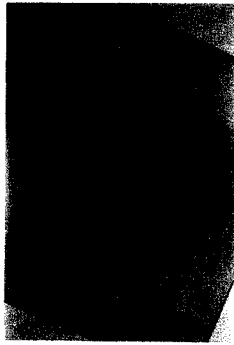


Fig. 2. Intrarenal distribution of ^{125}I -radioactivity in the nonfiltering kidney determined by X-ray film autoradiography. COR, cortex; OMO, outer stripe of outer medulla; OMI, inner stripe of outer medulla; IM, inner medulla. See details under Materials and Methods.

medulla, which was comparable with the results obtained by the tissue sampling method (Fig. 1).

The paraffin sections obtained from the same preparations of X-ray autoradiographic study were also exposed to the nuclear track emulsion and stained with hematoxylin-eosin to allow investigation of the intrarenal distribution of ^{125}I -EGF binding sites histologically (Fig. 3). The results of the grain counting are summarized in Table II. In the proximal straight tubules, the grain density on the antiluminal plasma membrane was 2.5 times higher than that on the intracellular space (Fig. 3A, Table II). The grain density on the luminal membrane was below one-fifth of that in the intracellular space. The grains were also distributed around the cortical collecting ducts (CCD) to the same extent as the proximal straight tubule (PST) (Fig. 3A, Table II). But the grain densities around the glomeruli and distal tubules were very low and, in fact, close to the background level. On the other hand, the grains were broadly distributed over the whole outer medulla and were not quantified because of the difficulty in histologically identifying each nephron segment in the outer medulla (Fig. 3B). Within the inner medulla, the silver grains were localized around both the inner medullary collecting ducts (IMCD) and the thin limb of Henle in the inner medulla (IMTLH). The grain density in the IMTLH was the highest in the whole kidney.

DISCUSSION

Using the isolated perfused rat kidney, we previously demonstrated that EGF receptors on the antiluminal plasma membrane have an important role in the renal uptake of EGF (1,5). Because kidney is composed of several heterogeneous tubules, which differ in function and morphology, it is necessary to know the distribution and relative densities of EGF receptors along the nephron. We therefore investigated the intrarenal localization of EGF-binding sites in the nonfiltering kidney by autoradiography. The nonfiltering kidney is appropriate for investigating the intrarenal distribution of EGF binding sites on the antiluminal plasma membrane, in which EGF can access only receptors on the antiluminal membrane side.

^{125}I -EGF radioactivity was distributed over the whole kidney, and was most highly concentrated in the inner medulla (Fig. 1). The fact that the binding of tracer ^{125}I -EGF was almost completely inhibited by the addition of 20 nM unlabeled EGF in the perfusate implies a specific binding of ^{125}I -EGF to its receptor on the antiluminal membrane. When 0.5 nM unlabeled EGF was added to the perfusate, the degree of inhibition in ^{125}I -EGF binding was less remarkable in the inner medulla than in the cortex or outer medulla, which suggests the presence of lower-affinity EGF binding in the inner medulla. The conclusion that the receptor densities are highest in the inner medulla, however, should be drawn with caution, since it is possible that the tissue-associated radioactivities may have arisen partly from degraded products which were produced on the antiluminal membrane by peptidergic enzymes and were locally taken up.

The intrarenal distribution of ^{125}I -EGF binding determined by autoradiography was also comparable with the results from the tissue sampling method (Fig. 1, Table I). Sites with high and low optical densities were observed within the cortex (Table I, Fig. 2). We therefore attempted to identify these ^{125}I -EGF binding sites morphologically by a tissue staining method. In the PST, the silver grains on the antiluminal membrane were determined separately from those in the intracellular space (Fig. 3A). Concerning the other sites except the PST, we counted the silver grains on the whole cell because of difficulty in distinguishing the intracellular space from the plasma membrane (Table II, Fig. 3). In the

Table I. Intrarenal Distribution of ^{125}I -EGF in the NFK^a

Expt	Cortex (% of dose/g tissue)			Outer medulla (% of dose/g tissue)			IM (% of dose/g tissue)
	Whole cortex	High	Low	Whole OM	OMO	OMI	
1	4.35	5.05	3.96	4.19	3.98	4.61	6.20
2	4.33	4.75	3.98	4.28	4.12	4.59	6.97
Mean	4.34	4.90	3.97	4.24	4.05	4.60	6.59

^a After the recirculatory perfusion of tracer ^{125}I -EGF for 20 min, the nonfiltering kidney was fixed by the perfusion of 2% glutaraldehyde. Paraffin sections (20 μm thick) were developed and fixed, and then the densities of enlarged autoradiographic images were measured with an image analyzer (IBAS, Carl Zeiss, Germany). The radioactivity localized to each tissue fraction was normalized by the tissue weight and the total radioactivity (dose) added to the perfusate. High, the higher distribution area of grain within the cortex; low, the lower distribution area of grain within the cortex; OM, outer medulla, OMO, outer stripe of outer medulla; OMI, inner stripe of outer medulla; IM, inner medulla.



Fig. 3. Morphologic demonstration of ¹²⁵I-EGF binding sites in the nonfiltering kidney. (A) The cortex, where the proximal straight tubule (1), glomeruli (2), cortical collecting ducts (3), and distal tubule (4) are shown. (B) The outer medulla. (C) The inner medulla, where the collecting duct (1) and thin limb of Henle (2) are indicated.

PST, the density of grains in the intracellular space was approximately 50% of that on the antiluminal plasma membrane. These data, obtained at 20 min after the recirculatory perfusion of ¹²⁵I-EGF in the nonfiltering kidney, indicate that ¹²⁵I-EGF internalization occurred from the antiluminal membrane to the intracellular space.

Using isolated nephron segments, EGF receptors have been shown to exist on the plasma membranes of the cortical collecting duct (16), proximal tubules (14), mesangial cells (15), and inner medullary collecting ducts (24). In the present study, the relatively high levels of EGF binding sites accessible from the antiluminal side were identified on PST, IMCD, and IMLH (Table II). But the levels of silver grains around the glomeruli were close to background level (Table II). This result does not necessarily contradict that of a previous study (15) which illustrated the existence of EGF receptors on the mesangial cells. Those studies have identified EGF receptors on various isolated nephron segments based on binding assays or the observation of the biological effects of EGF on those nephron segments but did not determine the relative distribution of EGF receptor density along the nephron. In contrast, the methodology used in the present study can estimate the relative distribution of EGF receptors in the kidney. The receptor density around the glomeruli was thus found to be relatively low.

Most recently, Breyer *et al.* (25) demonstrated the distribution and relative density of EGF receptors along the nephron using microdissected nephron segments isolated from rabbit kidney. Based on mapping studies, they showed that specific ¹²⁵I-EGF binding was highest in the PST, followed by the proximal convoluted tubules (PCT), CCD, IMCD, outer medullary collecting ducts (OMCD), and distal tubules (DT). They also observed specific ¹²⁵I-EGF binding to glomeruli. However, it is not known whether the EGF binding sites identified by using those isolated nephron segments were located on the antiluminal membrane or on the luminal membrane, while in our system using the nonfiltering kidney, the ligand can have access to the receptors only from the antiluminal side. Our results thus identified antiluminal EGF binding sites in the PST, CCD, IMCD, and DT. The high level of ¹²⁵I-EGF binding was identified on the IMLH.

What is the physiological role of EGF receptors located on the antiluminal membrane of the kidney? According to the studies using isolated nephron segments, EGF induced a decrease in glomerular filtration (15), the stimulation of phosphorylation in the rat proximal tubules (14), and the inhibition of sodium and water transport in the rabbit cortical collecting duct (16). In addition, our previous studies have demonstrated that the RME of EGF through the antiluminal

Table II. Histological Localization of Binding Sites of ¹²⁵I-EGF^a

	Cortex			IM	
	PST	Glo	CCD	TLH	CD
Whole		0.03 ± 0.01	0.32 ± 0.07	2.56 ± 0.31	1.11 ± 0.09
ALM	1.01 ± 0.17	ND	ND	ND	ND
Cell	0.40 ± 0.10	ND	ND	ND	ND
LM	0.07 ± 0.02	ND	ND	ND	ND

^a Grain number per unit area was determined. After the recirculatory perfusion of tracer ¹²⁵I-EGF for 20 min, the nonfiltering kidney was fixed by the perfusion of 2% glutaraldehyde solution. To observe the binding sites of ¹²⁵I-EGF histologically, paraffin sections (4 μm in thickness) were mounted on glass slides and dipped into the nuclear track emulsion and exposed for 60 days. After the preparations were developed and fixed, they were stained with hematoxylin-eosin and silver grains were counted using an image analyzer. IM, inner medulla; PST, proximal straight tubule; Glo, glomeruli; CCD, cortical collecting duct; TLH, thin limb of Henle; CD, collecting duct; ALM, antiluminal membrane; LM, luminal membrane.

plasma membrane plays an important role in the clearance of circulating plasma EGF (1,5), though its contribution to the total-body clearance was smaller than that of the liver. Therefore, it can be postulated that the EGF receptors located on the antiluminal membrane may play a role in the regulation of plasma endogenous EGF as clearance receptor. Recently, Maack *et al.* (26) upheld that the majority of the renal receptors of atrial natriuretic factor (ANF) serve as clearance receptors involved in the metabolic clearance and plasma homeostasis of endogenous ANF. RME of EGF from the antiluminal to the luminal direction by Madin-Darby canine kidney cells was also noted (27), again supporting the possibility that the EGF receptor serves in the clearance of circulating EGF.

Recent studies identified high levels of mRNA for prepro-EGF and EGF immunoreactivity localized on the luminal membrane of the cortical thick ascending limb and distal convoluted tubule (6,28). EGF and prepro-EGF are thought to be continuously released into the urine and may serve in urinary tract repair (29). Therefore, EGF receptors located on the antiluminal plasma membrane identified by the present study may not be accessible to the luminal endogenous EGF synthesized in the kidney, but only to the endogenous EGF released into the circulating plasma after synthesis in organs other than the kidney.

REFERENCES

1. Y. Sugiyama, D. C. Kim, H. Sato, S. Yanai, H. Satoh, T. Iga, and M. Hanano. Receptor-mediated disposition of polypeptides: Kinetic analysis of the transport of epidermal growth factor as a model peptide using in vitro isolated perfused organs and in vivo system. *J. Control. Release* 13:157-174 (1990).
2. Y. Sugiyama, H. Sato, S. Yanai, D. C. Kim, S. Miyauchi, Y. Sawada, T. Iga, and M. Hanano. Receptor-mediated hepatic clearance of peptide hormones. In D. D. Breimer, D. J. A. Crommelin, and K. K. Midha (eds.), *Topics in Pharmaceutical Sciences*, Amsterdam Medical Press, Amsterdam, 1989, pp. 429-443.
3. D. C. Kim, Y. Sugiyama, H. Sato, T. Fuwa, T. Iga, and M. Hanano. Kinetic analysis of in vivo receptor-dependent binding of human epidermal growth factor by rat tissues. *J. Pharm. Sci.* 77:200-207 (1988).
4. D. C. Kim, Y. Sugiyama, T. Fuwa, S. Sakamoto, T. Iga, and M. Hanano. Kinetic analysis of the elimination process of human epidermal growth factor in rats. *Biochem. Pharmacol.* 38:241-249 (1989).
5. D. C. Kim, Y. Sugiyama, Y. Sawada, and M. Hanano. Renal tubular handling of p-aminohippurate and epidermal growth factor in the filtering and nonfiltering perfused rat kidneys. *Pharm. Res.* (accepted for publication).
6. L. B. Rall, S. James, I. B. Graeme, G. I. Bell, R. J. Crawford, J. D. Penschow, H. D. Niall, and J. P. Coghlan. Mouse preproepidermal growth factor synthesis by the kidney and other tissues. *Nature* 313:228-231 (1985).
7. Y. Hirata and D. N. Orth. Epidermal growth factor (urogastrone) in human fluids: size heterogeneity. *J. Clin. Endocrinol. Metab.* 48:673 (1979).
8. E. C. Salido L. Barajas, J. Lechago, N. P. Laborde, and D. A. Fisher. Immunocytochemical localization of epidermal growth factor in mouse kidney. *J. Histochem. Cytochem.* 34:1155-1160 (1986).
9. L. Raaberg, E. Nexø, J. Damsgaard Mikkelsen, and S. Seier Poulsen. Immunohistochemical localization and development aspects of epidermal growth factor in the rat. *Histochemistry* 89:351-356 (1988).
10. P. S. Olsen, E. Nexø, S. Seier Poulsen, H. F. Hansen, and P. Kirkegaard. Renal origin of rat urinary epidermal growth factor. *Regul. Pept.* 10:37-45 (1984).
11. P. R. Goodyer, E. Kachra, C. Bell, and R. Rozen. Renal tubular cells are potential targets for epidermal growth factor. *Am. J. Physiol.* 255 (*Renal Fluid Electrolyte Physiol.* 24):F1191-F1196 (1988).
12. E. Sack and Z. Talor. High-affinity binding sites for epidermal growth factor (EGF) in renal membranes. *Biochem. Biophys. Res. Comm.* 154:312-317 (1988).
13. D. C. Kim, Y. Sugiyama, T. Iga, and M. Hanano. Kinetic analysis of clearance of epidermal growth factor in isolated perfused rat kidney. *Am. J. Physiol.* (in press).
14. R. C. Harris and T. O. Daniel. Epidermal growth factor binding, stimulation of phosphorylation, and inhibition of gluconeogenesis in rat proximal tubule. *J. Cell. Physiol.* 139:383-391 (1989).
15. R. C. Harris, R. L. Hoover, H. R. Jacobson, and K. F. Badr. Evidence for glomerular actions of epidermal growth factor in the rat. *J. Clin. Invest.* 82:1028-1039 (1988).
16. V. M. Vehaskari, K. S. Hering-Smith, D. W. Moskowitz, I. D. Weiner, and L. L. Hamm. Effect of epidermal growth factor on sodium transport in the cortical collecting tubule. *Am. J. Physiol.* 256 (*Renal Fluid Electrolyte Physiol.* 25):F803-F809 (1989).
17. T. Oka, S. Sakamoto, K. I. Miyoshi, T. Fuwa, K. Yoda, M. Yamasaki, G. Tamura, and T. Miyake. Synthesis and secretion of human epidermal growth factor by *Escherichia coli*. *Proc. Natl. Acad. Sci. USA* 82:7212-7216 (1985).
18. I. Vlodavsky, K. B. Kenneth, and G. Denis. A comparison of the binding of epidermal growth factor to cultured granulosa and luteal cells. *J. Biol. Chem.* 253:3744-3750 (1978).
19. N. Itoh, Y. Sawada, Y. Sugiyama, T. Iga, and M. Hanano. Kinetic analysis of rat renal tubular transport based on multiple indicator dilution method. *Am. J. Physiol.* 251 (*Renal Fluid Electrolyte Physiol.* 20):F103-F114 (1986).
20. F. H. Epstein, J. T. Brosnan, J. D. Tange, and B. D. Ross. Improved function with amino acids in the isolated perfused kidney. *Am. J. Physiol.* 243 (*Renal Fluid Electrolyte Physiol.* 12):F284-F292 (1982).
21. T. Maack. Renal clearance and isolated kidney perfusion techniques. *Kidney Int.* 30:142-151 (1986).
22. S. T. Kan and T. Maack. Transport and catabolism of parathyroid hormone in isolated rat kidney. *Am. J. Physiol.* 233 (*Renal Fluid Electrolyte Physiol.* 2):F445-F454 (1977).
23. J. J. M. Bergeron, R. Rachubinski, N. Searle, D. Borts, R. Sikstrom, and B. I. Posner. Polypeptide hormone receptors in vivo: Demonstration of insulin binding to adrenal gland and gastrointestinal epithelium by quantitative radioautography. *J. Histochem. Cytochem.* 28:824-835 (1980).
24. R. C. Harris. Response of rat inner medullary collecting duct to epidermal growth factor. *Am. J. Physiol.* 256 (*Renal Fluid Electrolyte Physiol.* 25):F1117-F1124 (1989).
25. M. D. Breyer, R. Redha, and J. A. A. Breyer. Segmental distribution of epidermal growth factor binding sites in rabbit nephron. *Am. J. Physiol.* 259 (*Renal Fluid Electrolyte Physiol.* 28):F553-F558 (1990).
26. T. Maack, M. Suzuki, F. A. Almedia, D. Nussenzweig, and R. M. Scarborough. Physiological role of silent receptors of atrial natriuretic factor. *Science* 238:675-668 (1987).
27. E. Maratos-Flier, C. Y. Y. Kao, E. M. Verdin, and G. L. King. Receptor-mediated vectorial transcytosis of epidermal growth factor by Madin-Darby canine kidney cells. *J. Cell Biol.* 105:1595-1601 (1987).
28. E. C. Salido, P. H. Yen, L. J. Shapiro, D. A. Fisher, and L. Barajas. In situ hybridization of prepro-epidermal growth factor mRNA in the mouse kidney. *Am. J. Physiol.* 256 (*Renal Fluid Electrolyte Physiol.* 25):F632-F638 (1989).
29. D. Fisher, E. Salido, and L. Barajas. Epidermal growth factor and the kidney. *Annu. Rev. Physiol.* 51:67-80 (1989).